Journal of Electroanalytical Chemistry 823 (2018) 47–53

Contents lists available at ScienceDirect

Journal of Electroanalytical Chemistry

journal homepage: www.elsevier.com/locate/jelechem

Effect of inter-electrode separation in the fabrication of nanoporous alumina by anodization

Marta Michalska-Domańska[a,b,*], Wojciech Jerzy Stępniowski[c,d], Marco Salerno[e]

[a] Institute of Optoelectronics, Military University of Technology, 2 Urbanowicza Str., 00-908 Warsaw, Poland
[b] Delft University of Technology, Department of Materials Science and Engineering, Faculty 3mE, Mekelweg 2, CD, Delft, Netherlands
[c] Department of Advanced Materials and Technologies, Faculty of Advanced Technology and Chemistry, Military University of Technology, 2 Urbanowicza Str., 00 908 Warszawa, Poland
[d] Department of Materials Science and Engineering, Lehigh University, Bethlehem, PA 18015, USA
[e] Istituto Italiano di Tecnologia, Materials Characterization Facility, via Morego 30, 16163 Genova, Italy

ARTICLE INFO

Keywords:
Anodization
Anodic aluminum oxide
Nanopores
Scanning electron microscopy
Image analysis
Regularity ratio
Electrode separation

ABSTRACT

The effect of the separation between electrodes on the main output parameters of the anodic aluminum oxide structure, namely the pore size, the cell size, the thickness and the regularity ratio was investigated. Pure aluminum foils were anodized in 0.3 M oxalic acid at different combinations of electrode separations (1.5, 3 and 6 cm), anodization voltages (30, 45 and 60 V) and temperatures (10, 20 and 30 °C). Whereas cell size and thickness appeared to be independent on the electrode separation, minor effects emerged for the pore size and significant effects emerged for the regularity ratio. The latter decreased with electrode separation at the lowest anodization voltage, but increased for the other voltages, especially at intermediate value of 45 V. For the temperature series, the regularity ratio decreased with separation at highest and, mostly, lowest temperature, while increased at intermediate temperature. Therefore, in addition to the major fabrication parameters of anodization voltage, current density, temperature and electrolyte concentration, it appears that the electrode separation may also cause relevant effects on the pattern quality, which should be taken into account for careful control of this nanofabrication process.

1. Introduction

The porous nanostructure of anodic aluminum oxide (AAO), which is the key to the well know and documented corrosion protection and decoration applications of anodized aluminum [1], has been disclosed since almost a century [2] and has been challenging researchers for decades in the attempt of providing a deep understanding of its mechanism of formation [3–10]. This point is not yet clear, and new theories in the field have continued to appear in recent years [11,12]. The knowledge on the topic comes from the contributions of scientists from different disciplines, from physics to chemistry, from material science to industry engineering, which has not always contributed to universal and exact definitions even for the terminology. An example is the use of terms such as mild and hard anodizing, the latter of which [13] is often either undefined or misunderstood by several authors as being performed at high electric field rather than resulting into hard coating. A comprehensive review of aluminum anodizing history and interdisciplinary scenario may be found in the book by Runge [14]. In this frame, and given the emerging applications of AAO in the areas of nanofabrication [15,16], biomedicine and sensing [17,18] [19], each bit of additional experimental characterization about the efficacy of different anodizing parameters and related process efficiency is welcome.

Usually the main input parameters affecting the above response are the anodization voltage, the current density, the temperature, and the type of electrolyte and its concentration. However, in principle, the inter-electrode separation also may cause secondary though significant effects. In this work, the effect of changing the separation between the anode and cathode during anodization on the morphological AAO parameters was investigated. In particular the electrolyte type and concentration was fixed, and the electrode separation was varied in combination with either the voltage or the temperature, around central values of these variables. The pore pattern parameters of cell size (also identified in the literature as interpore distance) have been measured, together with oxide coating thickness. The regularity ratio, describing the pore pattern ordering, has also been calculated and discussed. The

* Corresponding author.
E-mail addresses: marta.michalska@wat.edu.pl, m.e.michalska-domanska@tudelft.nl (M. Michalska-Domańska), wojciech.stepniowski@wat.edu.pl, wos218@lehigh.edu (W.J. Stępniowski), marco.salerno@iit.it (M. Salerno).

https://doi.org/10.1016/j.jelechem.2018.05.038
Received 18 April 2018; Received in revised form 28 May 2018; Accepted 28 May 2018
Available online 29 May 2018

aim was not to provide a deeper understanding of the mechanism of anodization, but rather to assess the possible effects in the practice of an anodization parameter usually not considered in the research reports. The null hypothesis is that the inter-electrode separation does not affect the results significantly.

2. Materials and methods

2.1. AAO fabrication

The high purity aluminum foil (99.9995%, Alfa Aesar) of 250 μm thickness was cut into rectangular specimens (10 × 20 mm^2) and degreased in acetone and ethanol. Next, the specimens were electropolished in a mixture of ethanol and $HClO_4$ (1:4 vol.) at 10 °C with current density 0.5 A/cm^2 for 1 min, rinsed with ethanol, distilled water and blown dry in the air. The anodization was carried out in a two-electrode electrochemical cell with a platinum grid as the cathode and the aluminum specimen as the anode, consisting of a cylindrical jacketed beaker. A schematic representation of the experimental setup used for anodization experiments is shown in Fig. S1. The process was conducted in 500 mL of 0.3 M aqueous solution of oxalic acid at various voltages U (30, 45, 60 V) and temperatures T (10, 20, 30 °C) under vigorous magnetic stirring, with the same stirring speed for all experiments. For each sample the working surface of the specimen dipped in the electrolyte was kept constant and the separation s between the electrodes was changed among three values of 1.5, 3 and 6 cm. In a first step of anodization the surface layer of alumina was formed by 1 h and after that was removed by chemical etching in a mixture of 6 wt% phosphoric acid and 1.8 wt% chromic acid at 60 °C for 1 h. To obtain ordered nanoporous AAO, a second anodization step at the same set of operating conditions as used for the first step was performed, for 30 min. A DC power supply DF1760SL5A (NDN, Poland) was used to control the applied voltage.

Digital images of prepared AAO, both top-view and cross-sections, were made by field-emission scanning electron microscope (SEM) Quanta 3D FEG (FEI, OR, USA). The thickness of prepared AAO was estimated directly from cross sections images, based on at least five measurements ($N \geq 5$).

2.2. Design of the experiment

Three values of anodization voltage U (namely, 30, 45 and 60 V), three values of temperature T (namely, 10, 20 and 30 °C) and three values of electrode separation s (namely, 1.5, 3 and 6 cm) were considered. In the space of all the possible combinations of the above values ($3^3 = 27$), only a subset of selected combinations was considered for the present investigation. Basically, the parameter of major interest, s, was varied throughout all its three values only around a single central point of T or U, respectively. This selection is described in the space of the input anodization parameters in Fig. 1 as the filled circles, whereas the boundary combinations (not explored here) are represented by void circles. Actually, all the combinations of the two gray planes intersecting in the middle of the explored area in Fig. 1 have been analyzed.

2.3. Top view image analysis

The SEM images of the AAO surfaces, taken at 50,000× magnification, have 8-bit gray levels intensity and 1024 × 943 pixels. From these images, after segmentation with operator-selected threshold within the program ImageJ 1.37v (NIH, MD, USA) [20], the morphological parameters in the real (direct) space of pore size d and cell size D have been obtained. Additionally, the fast-Fourier transform (FFT) of the SEM images have been calculated by the program WSxM 5.0 (nanotech Electronica, Spain) [21]. The FFT images in the space of frequencies have 8-bit gray levels intensity and 400 × 400 pixels. From these images the representative mean radial profiles were extracted, by averaging at all angles. From each single image profile, the following quantity has been calculated, defined as the regularity ratio:

$$R = \frac{H}{W_{1/2}}\left(\frac{\sqrt{n}}{S^{1.5}}\right)$$

where H is the intensity at the FFT profile peak and $W_{1/2}$ is its FWHM; the rest of the expression in parentheses is the correction factor [22,23] accounting for the pores density of different AAO samples, with n the number of pores in the image and S the image area. The appropriateness of this correction factor has been discussed and validated in previous works [24].

The values of each output parameter extracted from the top-view SEM images (d, D and R) are means of the results from three different images ($N = 3$).

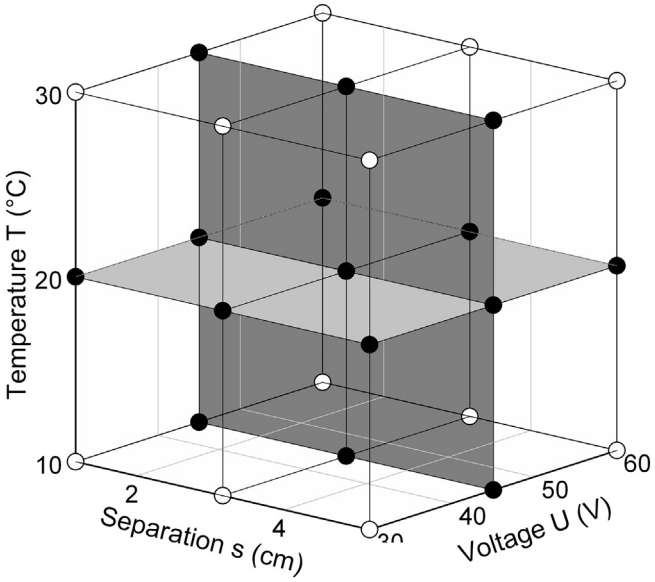

Fig. 1. Representation of the 3D space of input anodization parameters explored: the filled circles identify datapoint combinations investigated in this work, the void circle conditions have not been investigated.

3. Results

Raw SEM images of the AAO top surface resulting from the selected combinations of input parameters for the anodization are presented in Figs.2 and 3. These images represent the anodization conditions described by the central 'planes' of the space of parameters (gray planes in Fig. 1), i.e. the selected conditions at either constant T (= 20 °C) and constant U (= 45 V), in Figs. 2 and 3, respectively. The images shown are single cases representative of the respective surfaces. Imaging was repeated in three different regions of each sample, spaced apart of at least 3 mm, and similar results were observed without any appreciable apparent difference on visual inspection, as well as resulting analysis, as it appears from the comparatively small error bars in the plots of Figs. 4 and 5.

From the SEM images in Fig. 2 (i.e. with changing U and s at constant, intermediate T), the only clearly visible is the increase in pore spacing i.e. cell size D with increasing U (i.e. moving downward across the rows). Horizontally moving among the different s values does not show any evident effect. It also appears that the intermediate row (U = 45 V) exhibits the better defined domains of ordered (hexagonal packed) pore lattice. For this reason this voltage for the subsequent investigation of the influence of s on the morphology of AAO fabricated at the different T was chosen.

For the series in Fig. 3 (i.e. with changing T and s at constant, intermediate U), apparently no visible effect emerges in either direction